Synthesis and Structure−Activity Relationship of Small-Molecule Malonyl Coenzyme A Decarboxylase Inhibitors

Jie-Fei Cheng,*,† Mi Chen,† David Wallace,† Souvothy Tith,† Masayuki Haramura,† Bin Liu,† Chi Ching Mak,† Thomas Arrhenius,† Sean Reily,‡ Steven Brown,‡ Vicki Thorn,‡ Charles Harmon,‡ Rick Barr,§ Jason R. B. Dyck,§ Gary D. Lopaschuk,§ and Alex M. Nadzan†

Departments of Chemistry and Discovery Biology, Chugai Pharma USA, LLC., 6225 Nancy Ridge Drive, San Diego, California 92121, and Metabolic Modulator Research Ltd. (MMRL), 2020 Research Transition Facility, University of Alberta, Edmonton, Alberta, Canada

Received February 3, 2005

The discovery and structure−activity relationship of first-generation small-molecule malonyl-CoA decarboxylase (MCD; CoA = coenzyme A) inhibitors are reported. We demonstrated that MCD inhibitors increased malonyl-CoA concentration in the isolated working rat hearts. Malonyl-CoA is a potent, endogenous, and allosteric inhibitor of carnitine palmitoyltransferase-I (CPT-I), a key enzyme for mitochondrial fatty acid oxidation. As a result of the increase in malonyl-CoA levels, fatty acid oxidation rates were decreased and the glucose oxidation rates were significantly increased. Demonstration of in vivo efficacy of methyl 5-(*N*-(4-(1,1,1,3,3,3-hexafluoro-2-hydroxypropan-2-yl)phenyl)morpholine-4-carboxamido)pentanoate (**6u**) in a pig ischemia model indicated that MCD inhibitors may be useful for treating ischemic heart diseases.

Introduction

The enzyme malonyl-CoA decarboxylase (MCD, EC 4.1.1.9; CoA = coenzyme A) catalyzes the conversion of malonyl-CoA to acetyl-CoA and thereby regulates malonyl-CoA levels. MCD was first purified from the uropygial glands of waterfowl and subsequently from a number of mammalians, plants and bacteria.[1] Identification of patients with MCD deficiency led to the cloning of a human MCD gene that is highly homologous to the goose and rat genes.[2] A single human MCD mRNA is observed by Northern blot analysis. The highest mRNA expression levels are found in muscle and heart tissues, followed by liver, kidney and pancreas, with detectable amounts found in many other tissues. Recent studies indicate that MCD exists in cytosolic, mitochondrial, and peroxisomal compartments.[1h,2b,3,4]

Malonyl-CoA is a potent endogenous inhibitor of carnitine palmitoyltransferase-I (CPT-I), an enzyme essential for the mitochondrial metabolism of long-chain fatty acids. CPT-I is the rate-limiting enzyme in fatty acid oxidation and catalyzes the formation of acylcarnitine, which is transported from the cytosol across the mitochondrial membranes by acylcarnitine translocase. Inside the mitochondria, the long-chain fatty acids are transferred back to their CoA compounds by a complementary enzyme, CPT-II, where acyl-CoA enters the β-oxidation pathway generating acetyl-CoA. In the liver, high levels of acetyl-CoA lead to elevated malonyl-CoA levels, which inhibit CPT-I, thereby preventing fatty acid oxidation and favoring fatty acid synthesis. Conversely, low malonyl-CoA levels favor fatty acid oxidation by allowing the transport of long-chain fatty acids into the mitochondria. Therefore, malonyl-CoA is a central metabolite that plays a key role in balancing fatty acid synthesis and fatty acid oxidation.[5] In skeletal and cardiac muscle, where fatty acid synthesis rates are low, we and others hypothesized that the role of malonyl-CoA and MCD in these tissues is to regulate fatty acid metabolism via inhibition of the muscle form of CPT-I, which is more sensitive than the liver form of CPT-1 (IC_{50} of 0.03 vs 2.5 μM).[6]

In the heart, fatty acid oxidation is a major source of energy and fatty acid uptake and metabolism in the heart down-regulate glucose metabolism. The regulation of intermediary metabolism by serum levels of fatty acid and glucose comprises the glucose−fatty acid cycle ("Randle cycle").[7] Under ischemic conditions, limited oxygen supply reduces both fatty acid and glucose oxidation and reduces the amount of ATP produced by oxidative phosphorylation in the cardiac tissues. Glycolysis increases in an attempt to maintain ATP levels, although a consequence of this is a buildup of lactate and a drop in intracellular pH. Energy is spent maintaining ion homeostasis, and myocyte cell death occurs as a result of abnormally low ATP levels and disrupted cellular osmolarity. The problem is complicated by a decrease in malonyl-CoA levels in the heart due to an activation of AMP-activated protein kinase (AMPK), which phosphylates and thus inactivates acetyl-CoA carboxylase (ACC). This increases CPT-I activity, and fatty acid oxidation is favored over glucose oxidation.

A number of clinical and experimental studies indicate that shifting energy metabolism in the heart toward glucose oxidation is an effective approach to decreasing the symptoms associated with myocardial ischemia.[8,9] Certain antianginal drugs such as ranolazine (*N*-(2,6-dimethylphenyl)-2-[4-[2-hydroxy-3-(2-methoxyphenoxy)propyl]piperazin-1-yl]ethanamide) inhibit fatty acid β-oxidation and stimulate glucose oxidation.[10] Trimetazidine (1-[(2,3,4-trimethoxyphenyl)methyl]piperazine) has been shown to specifically inhibit the long-chain 3-ketoactyl CoA thiolase (3-KAT), an essential step in fatty acid oxidation.[11] Inhibiting CPT-I activity through increasing malonyl-CoA levels with MCD inhibitors would result in a novel and perhaps a much safer method, compared to other known small-molecule CPT-I inhibitors, to the prophylaxis and treatment of ischemic heart diseases (Figure 1).[12]

Two metabolic complications commonly associated with diabetes are hepatic overproduction of ketone bodies and organ toxicity associated with sustained elevated levels of glucose. Malonyl-CoA inhibition of CPT-I is an important regulatory mechanism that controls the rate of fatty acid oxidation during

* To whom correspondence should be addressed. Phone: 858-622-7029. Fax: 858-558-9383. E-mail: jcheng@trlusa.com. Present Address: Tanabe Research Lab USA, Inc., 4540 Towne Centre Court, San Diego, CA 92121.
† Department of Chemistry, Chugai Pharma USA, LLC.
‡ Department of Discovery Biology, Chugai Pharma USA, LLC.
§ University of Alberta.

10.1021/jm050109n CCC: $33.50
Published on Web 02/11/2006

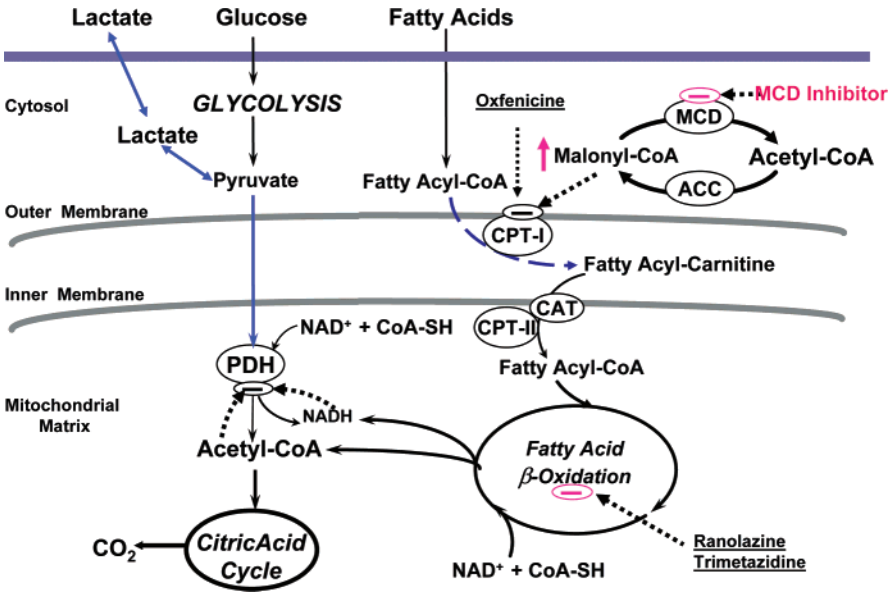

Figure 1. Malonyl-CoA regulation of energy metabolism.

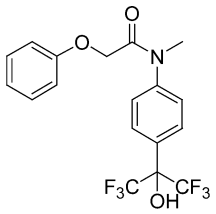

1

Figure 2. Initial HTS hit.

the onset of the hypoinsulinemic−hyperglucagonemic state. Stimulation of glucose oxidation rate via inhibition of fatty acid oxidation may have the potential to regulate blood-glucose levels and ameliorate some symptoms of type II diabetes. Several irreversible and reversible CPT-I inhibitors that have been evaluated for their ability to control blood glucose levels were found to be invariably hypoglycemic.[13] However, stimulation of fatty acid oxidation through knockout of the ACC2 (ACCβ)[14] gene or overexpression of the hepatic MCD[15] protein was found to improve insulin sensitivity, indicating the complex nature of the metabolic pathway.

On the basis of the rationale illustrated above, we speculated that increasing the malonyl-CoA level in tissues has potential use in heart disease and diabetes therapy. We therefore established a high-throughput screening assay and used it to screen an in-house compound library employing either MCD from rat hearts or MBP-fused human MCD protein (MBP = maltose-binding protein).[16] Using this paradigm, we discovered a number of small-molecule MCD inhibitors, one of them possessing the phenylhexafluoroisopropanol[17] moiety (**1**, Figure 2). The hexafluoroisopropanol moiety of compound **1** was found to be essential for the high in vitro MCD inhibitory activity (vida infra). The structure−activity relationship (SAR) studies on this initial hit led to the identification of a series of MCD inhibitors that not only exhibit potent in vitro MCD inhibitory activities and favorable pharmacokinetic properties but also exhibit excellent efficacy in regulating energy metabolism in isolated working rat hearts.

Chemistry

The synthesis of amide and urea derivatives of **1** is outlined in Scheme 1. The key intermediate **4** was prepared either through

Scheme 1. Synthesis of *p*-[2-Hydroxy-(1,1,1,3,3,3-hexafluoro-2-propyl)]aniline Derivatives[a]

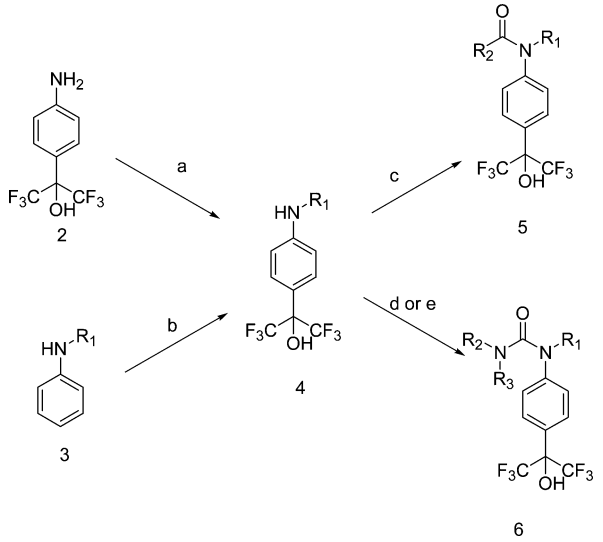

[a] Reagents and conditions: (a) alkyl halide, Et_3N, DCM; (b) $CF_3COCF_3 \cdot 6H_2O$, molecular sieves, toluene, 60−80 °C; (c) R_2COCl, poly(4-vinylpyridine), DCM; or R_2COOH, EDAC, DMAP, DMF; (d) R_2NCO, poly(4-vinylpyridine), DCM; (e) $COCl_2$, DIPEA, toluene and then R_2R_3NH, 80−100 °C.

alkylation of commercially available 2-(4-aminophenyl)-1,1,1,3,3,3-hexafluoropropan-2-ol (**2**) or through Friedel−Craft type alkylation of substituted aniline **3** with hexafluoroacetone hydrate in the presence of molecular sieves or an acid such as *p*-toluenesulfonic acid.[18] The reaction went smoothly, giving rise predominantly to the para-substituted product (**4**) in excellent yields. Reaction of **4** with acyl chloride, anhydride, or carboxylic acid afforded the amide derivatives **5**. Similarly, the reaction of **4** with isocyanates provided trisubstituted ureas. The tetrasubstituted ureas were prepared in a stepwise fashion. Intermediate **4** was first treated with phosgene/triphosgene to provide the corresponding carbamoyl chlorides, which upon treatment with 2 equiv of a secondary amine in toluene at 80 °C afforded the desired tetrasubstituted ureas **6** in modest to good yields.

The meta-substituted isomer of the initial hit **1** was prepared in a different fashion, as shown in Scheme 2. According to the

Scheme 2. Synthesis of *m*-[2-Hydroxy-(1,1,1,3,3,3-hexafluoro-2-propyl)]aniline Derivative[a]

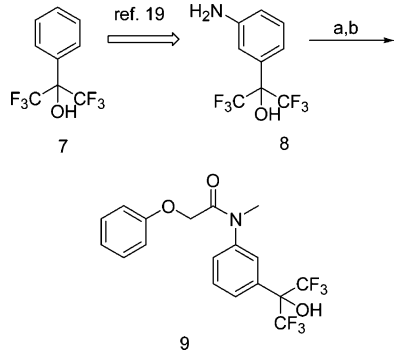

[a] Reagents and conditions: (a) $PhOCH_2COCl$, Et_3N, DCM, room temp; (b) MeI, NaH, THF, 0 °C to room temp.

Scheme 3. Synthesis of *p*-[2-Hydroxy-(1,1,1,3,3,3-hexafluoro-2-propyl)]benzoic Acid Amides[a]

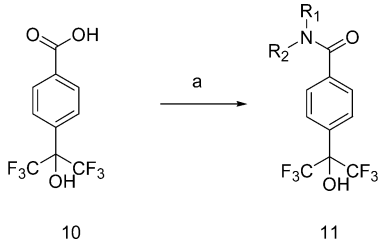

[a] Reagents and conditions: (a) R_1R_2NH, CDI, THF.

literature procedure,[19] 2-hydroxy-1,1,1,3,3,3-hexafluoropropylbenzene **7** was nitrated with fuming nitric acid in sulfuric acid to provide the corresponding *m*-nitro derivative, which was further reduced with iron to the desired aniline compound **8**. Acylation with phenoxyacetyl chloride followed by methylation with MeI in the presence of NaH afforded the desired regioisomer **9**.

Scheme 3 illustrates the synthesis of a series of 4-(2,2,2-trifluoro-1-hydroxy-1-trifluoromethylethyl)benzoic acid amide derivatives **11**. To distinguish these amides with the ones mentioned above, we designated 4-(2,2,2-trifluoro-1-hydroxy-1-trifluoromethylethyl)benzoic acid amide as reverse amides. These reverse amides were prepared efficiently by conventional peptide coupling methods from commercially available 4-(2,2,2-trifluoro-1-hydroxy-1-trifluoromethylethyl)benzoic acid **10**. Most preparations did not require a chromatographic purification.

Results and Discussion

All compounds prepared were tested initially for their ability to inhibit rat heart MCD (data not shown) as well as the soluble form of recombinant MBP fusion protein (MBP-hMCD) as described elsewhere and in the Experimental Section.[16] An initial attempt to replace the hexafluoroisopropanol moiety was unsuccessful. Removal of one of two trifluoromethyl groups or the hydroxyl group resulted in a significant or complete loss of MCD inhibitory activity (data not shown). Replacement of the hydroxyl group with methoxy also led to an inactive compound. The regioisomer of initial hit **1** (e.g., compound **9**) is also inactive. The lead optimization was therefore performed in terms of in vitro enzyme inhibitory activity, in vitro pharmaceutical properties (solubility, liver microsome stability, and Caco-2 permeability), and ex vivo efficacy in isolated working rat hearts using the 2-hydroxy-1,1,1,3,3,3-hexafluoro-2-propylphenyl scaffold as a core structure.

As shown in Table 1, *N*-alkyl-*N*-(1,1,1,3,3,3-hexafluoro-2-hydroxylpropylphenyl)amides exhibited a higher potency in the

Table 1. Amide-based MCD Inhibitors

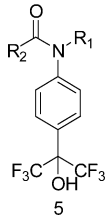

compd	R_1	R_2	IC_{50} (nM)[a]
1	−Me	$PhOCH_2$−	930
5a	−H	$PhOCH_2$−	6626
5b	−H	$PhCH_2CH_2$−	4337
5c	−Me	$PhCH_2CH_2$−	773
5d	−Et	$PhCH_2CH_2$−	175
5e	−*i*-Pr	$PhCH_2CH_2$−	199
5f	−*n*-Bu	$PhCH_2CH_2$−	79
5g	$-CH_2COOMe$	$PhCH_2CH_2$−	105
5h	$-CH_2COOH$	$PhCH_2CH_2$−	376
5i	−Bn	$PhCH_2CH_2$−	580
5j	−cyclohexyl	$PhCH_2CH_2$−	150
5k	−H	*i*-Pr−	NA[b]
5l	−Me	*i*-Pr−	178
5m	−Me	3-Py−	1015
5n	−Me	4-Py−	394
5o	−Et	*i*-Pr−	41
5p	−*n*-Pr	*i*-Pr−	28
5q	−*n*-Bu	*i*-Pr−	20
5r	$-CH_2CH_2NMe_2$	*i*-Pr−	1147
5s	$-CH_2CH_2OH$	*i*-Pr−	106
5t	$-CH_2COOMe$	*i*-Pr−	34
5u	$-CH_2COOH$	*i*-Pr	627
5v	$-(CH_2)_4COOMe$	*i*-Pr	26
5w	$-(CH_2)_4COOH$	*i*-Pr	8
5x	$-(CH_2)_4$−(5-1*H*-tetrazole)	*i*-Pr	8
5y	$-(CH_2)_4CN$	*i*-Pr	20
5z	−Et	−*p*-CNPh	37
5aa	−Et	−4-Py	95

[a] Data are reported as the mean of $n \geq 3$ determinations. SD was generally ±20% of the average. [b] Not active at 10 μM.

in vitro enzyme assay compared to their nonalkylated counterparts. Compounds **5a**, **5b**, and **5k** inhibited MCD enzyme at high micromolar concentrations. A methyl group at the nitrogen atom increased potency by 6−80 times. It is well-known that the stable conformation of an aniline amide in solution, as well as in the crystal form, is highly dependent on the nature of the substituents on the amide nitrogen atom, with the cis conformation being preferred in an *N*-alkylanilides and with the trans conformation being preferred in a nonsubstituted acetanilide.[20] It is therefore assumed that the active conformation of initial hit **1**, or similar amide compounds, is a cis conformation. The amide carbonyl group may also play a role as a hydrogen bond acceptor, since the corresponding tertiary amines or ether compounds did not exhibit significant MCD inhibitory activities (data not shown). The chain length of the alkyl group on the nitrogen atom greatly affects the potency as well (**5c**−**e**).

N-Alkyl-*N*-(1,1,1,3,3,3-hexafluoro-2-hydroxypropylphenyl)-amides generally are highly hydrophobic. To improve properties of these hydrophobic compounds, especially the improvement of solubility, a terminal carboxylic acid or hydroxyl group was introduced into some compounds. This did not adversely affect the ability of these compounds to inhibit MCD. However, a basic group such as the *N*,*N*-dimethylamino group at the terminal position significantly decreased the potency (**5r**, IC_{50} = 1147 nM). Another significant observation in the amide series was the dramatic increase in potency through introduction of substitution at the α-position of the amide group. When the substituent on the nitrogen atom was larger than a methyl group,

Table 2. Urea-Based MCD Inhibitors

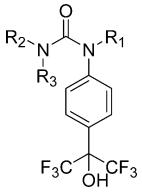

compd	R_1	R_2	R_3	IC_{50} (nM)[a]
6a	−H	Ph−	−H	NA[b]
6b	−Me	Ph−	−H	1564
6c	−H	$-CH_2CH_2OCH_2CH_2-$		NA[b]
6d	−Et	Me−	−Me	59
6e	−Et	Et−	$-(CH_2)_4OH$	60
6f	−Me	$-CH_2CH_2OCH_2CH_2-$		321
6g	−Et	$-CH_2CH_2OCH_2CH_2-$		74
6h	−*n*-Pr	$-CH_2CH_2OCH_2CH_2-$		34
6i	−*n*-Bu	$-CH_2CH_2OCH_2CH_2-$		30
6j	−*n*-pentyl	$-CH_2CH_2OCH_2CH_2-$		19
6k	−*n*-hexyl	$-CH_2CH_2OCH_2CH_2-$		31
6l	−*n*-heptyl	$-CH_2CH_2OCH_2CH_2-$		73
6m	−octyl	$-CH_2CH_2OCH_2CH_2-$		269
6n	$-CH_2CH_2Ph$	$-CH_2CH_2OCH_2CH_2-$		43
6o	$-CH_2CH_2OH$	$-CH_2CH_2OCH_2CH_2-$		166
6p	$-CH_2COOMe$	$-CH_2CH_2OCH_2CH_2-$		80
6q	$-CH_2CH_2COOMe$	$-CH_2CH_2OCH_2CH_2-$		99
6r	$-CH_2CH_2COOH$	$-CH_2CH_2OCH_2CH_2-$		247
6s	$-CH_2CH_2CH_2COOMe$	$-CH_2CH_2OCH_2CH_2-$		75
6t	$-(CH_2)_3CN$	$-CH_2CH_2OCH_2CH_2-$		40
6u	$-(CH_2)_4COOMe$	$-CH_2CH_2OCH_2CH_2-$		42
6v	$-(CH_2)_4COOH$	$-CH_2CH_2OCH_2CH_2-$		14

[a] Data are reported as the mean of $n \geq 3$ determinations. SD was generally ±20% of the average. [b] Not active at 10 μM.

the effect was much greater. Taken together, our data suggest that a small and branched aliphatic group such as an isopropyl group on the amide side and a 4-carbon to 5-carbon substitution on the nitrogen atom are preferred. 5-{Isobutyryl-[4-(2,2,2-trifluoro-1-hydroxy-1-trifluoromethylethyl)phenyl]amino}-pentanoic acid (**5w**) and its tetrazole analogue (**5x**) showed low nanomolar IC_{50} values (8 nM) against MCD.

A series of *N*,*N*′-disubstituted, trisubstituted and tetrasubstituted ureas based on the *p*-(1,1,1,3,3,3-hexafluoro-2-hydroxy)-propylaniline scaffold were prepared according to Scheme 1. As expected, tetrasubstituted ureas were generally better MCD inhibitors compared to the corresponding trisubstituted or disubstituted ones. *N*,*N*′-Disubstituted ureas (e.g., **6a**, Table 2) were essentially inactive against the MCD enzyme. Depending on the substitution pattern, trisubstituted ureas showed either poor inhibitory activity (**6b**) or no activity at all (**6c**). Most tetrasubstituted ureas, except diaryl ones, generally exhibited good inhibitory activity. As shown in Table 2 and seen in the amide series, linear aliphatic chains, with up to five carbons, on the nitrogen atom (**6f**−**m**) were preferable. Small aliphatic substituents were also preferred, with morpholinylurea derivatives (**6f**−**v**) consistently demonstrating great solubility and metabolic stability enhancement. Terminal carboxylic acid or other hydrophilic groups were well-tolerated, with compound **6v** exhibiting the highest potency (IC_{50} = 14 nM).

Reverse amides **11** (Table 3) inhibited MCD enzyme activity in the in vitro MCD enzyme assay, but the potency was far lower than the potency of amide compounds mentioned above. A notable exception was those compounds with two small-branched aliphatic chains, which exhibited a submicromolar or nanomolar inhibition (e.g., compound **11i**, IC_{50} = 70 nM). Besides the low potency, these compounds also tended to be

Table 3. In Vitro Data for Reversed Amides

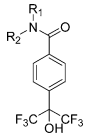

11

compd	R_1	R_2	IC_{50} (μM)[a]
11a	$PhCH_2CH_2$	H	2.65
11b	$PhCH_2CH_2$	Me	1.99
11c	Bn	Me	1.00
11d	OCH_3	Me	1.45
11e	$-CH_2CH_2CH_2CH_2-$		0.85
11f	$-CH_2CH_2OCH_2CH_2-$		1.14
11g	$-CH_2CH_2CH_2CH_2CH_2-$		0.98
11h	$NCCH_2CH_2$	Et	0.29
11i	*i*-Bu	*i*-Bu	0.07

[a] Data are reported as the mean of $n \geq 3$ determinations. SD was generally ±20% of the average.

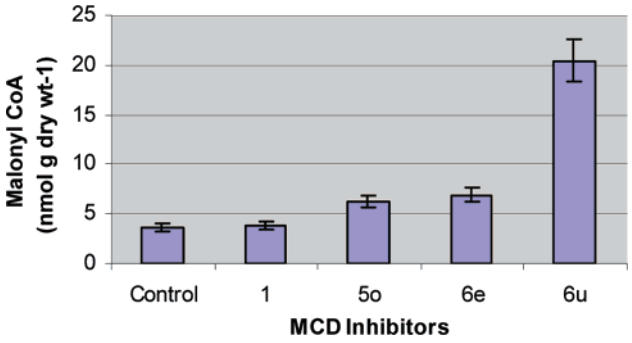

Figure 3. Malonyl-CoA content in the isolated working rat hearts (n = 8) in the absence and presence of MCD inhibitors: (**1**) 50 μM; (**5o**, **6e**, **6u**) 20 μM.

metabolized quickly in the in vitro liver microsome stability test (data not shown).

Measurement of Malonyl-CoA Content. According to our hypothesis illustrated in Figure 1, isolated working rat hearts perfused with MCD inhibitors would demonstrate an elevation of malonyl-CoA level,[21] a decrease in fatty acid oxidation rates, and an increase in glucose oxidation rates. To test the hypothesis, a number of MCD inhibitors were selected on the basis of a number of in vitro properties, especially in vitro potency, solubility, and Caco-2 permeability, and were tested for their ability to regulate energy metabolism in the isolated working rat hearts.

The initial high-throughput screeing (HTS) hit compound **1**, with an IC_{50} of 0.93 μM, showed a marginal increase in malonyl-CoA levels in the isolated working rat heart tissue at a test concentration of 50 μM. However, amide compound **5o** and urea compound **6e**, with low-nanomolar in vitro MCD inhibitory activity, showed statistically significant increases in malonyl-CoA concentration at 20 μM (Figure 3). The most dramatic increase in malonyl-CoA was observed for the urea derivative **6u**, which demonstrated a 6-fold increase in MCA levels compared to the control condition (0.05% DMSO).

Glucose Oxidation in Isolated Working Heart. A set of MCD inhibitors was selected, and their effects on glucose oxidation rates in the isolated working rat hearts were measured.[22] These compounds exhibited 3−60 times more potent MCD inhibitory activities than the initial hit compound **1**. Compound **1** at 50 μM caused a 100% increase in glucose oxidation rate compared to the DMSO control. An MCD inhibitor with low potency and low permeability such as **5h**

Table 4. MCD Inhibitors and Glucose Oxidation Rate in Working Rat Hearts

compd	IC_{50} (μM)	solubility (PBS, pH 7.4) (μM)[a]	Caco-2 ($\times 10^{-6}$ cm/s)[b]	rat liver microsome (%)[c]	human liver microsome (%)[c]	GOX[d]
1	0.931	46	28.6	100	100	2.0[e]
5aa	0.095	59.8	54.4	86	97	2.47
5h	0.317	190.6	0.4	65	88	1.26
5n	0.394	136.2	41.0	88	98	2.58
5o	0.040	19.3	69.1	60	89	2.05
5s	0.106	199.5	52.0	76	85	1.90
5z	0.041	8.7	38.7	66	93	2.81
6e	0.061	187.3	49.4	7	51	2.42
6g	0.074	189.3	68.2	9	87	2.14
6u	0.041	166.9	32.9	1	95	3.86
6v	0.014	205.6	1.7	108	99	2.90
ranolazine						1.77[f]
trimetazidine						2.01[g]

[a] Solubility was measured using the HPLC method at pH 7.4 in PBS containing 1% DMSO. [b] Caco-2 permeability was determined at Cerep using standard protocol. [c] Percentage indicates the remaining of the test compound (5 μM) after 1 h of incubation at 37 °C and 1 mg of protein/mL of microsome. [d] Glucose oxidation rates (GOX) were calculated as a ratio of test compound (20 μM) to DMSO (0.05%) control. See Experimental Section for details. [e] 50 μM. [f] See ref 10a. [g] See ref 11.

tended to give a less profound effect on glucose oxidation rates. On the other hand, compound **6v** potently stimulated glucose oxidation even though it has low permeability. The high glucose oxidation rate induced by **6v** may be ascribed to its high potency. The effect of solubility on the glucose oxidation is less obvious partly because of the presence of a large amount of bovine serum albumin (BSA) in the perfusate. As can be seen in Table 4, most of MCD inhibitors showed better efficacy in stimulating glucose oxidation compared to ranolazine or trimetazidine.

Conclusions

On the basis of the initial hit obtained from HTS on an in-house compound library, a series of small-molecule MCD inhibitors with the *N*-alkyl(hexafluoroisopropyl)aniline scaffold were synthesized and optimized. *N*-Alkyl(hexafluoroisopropyl)-aniline amides and urea derivatives displayed potent in vitro inhibitory activity against the soluble form MBP-fused MCD protein. These compounds are also equally active against native MCD (data not shown).[16] The most potent inhibition was achieved by compounds **5w** and **6v** in either the amide or urea series with an IC_{50} of 8 and 14 nM, respectively. These potent MCD inhibitors generally contain small aliphatic chains on the nitrogen atom of α,α-disubstituted carboxyl groups or *N*,*N*-disubstituted ureido functions. The small aliphatic groups are also preferred at the α-position of the carboxyl group or on the nitrogen atom of the ureido group.

Selected compounds were further profiled in term of malonyl-CoA concentration and glucose oxidation rates in the isolated working rat heart model. Compounds **5o**, **6e**, and **6u** were demonstrated to increase malonyl-CoA content in the rat heart tissues compared to the control. The initial hit compound **1** was less efficacious compared to other more potent analogues. The ability to stimulate glucose oxidation rates in the isolated working rat hearts was also confirmed for a large number of compounds prepared on the basis of the initial hit **1** (cf. Table 4). A number of compounds showed 2- to 3-fold increases in glucose oxidation rate at 10−20 μM, which are comparable to or more potent than known metabolic modulators such as ranolazine and trimetazidine.

On the basis of the overall profile, including in vitro potency, solubility, pharmacokinetics (data not shown), and ex vivo activity in the isolated working rat heart, compound **6u** (CBM-300864) was chosen to be the first MCD inhibitor for proof-of-concept studies in an in vivo pig demand-induced ischemia model. By use of a pig model of demand-induced ischemia, **6u** significantly increased glucose oxidation rates and reduced lactate production compared with vehicle-treated hearts, which was accompanied by a significant increase in cardiac work compared with controls. These data show that MCD inhibitors, which increase myocardial malonyl-CoA levels,[12,23] decrease fatty acid oxidation and accelerate glucose oxidation in both ex vivo rat hearts and in vivo pig hearts. This switch in energy substrate preference improves cardiac function during and after ischemia, suggesting that pharmacological inhibition of MCD may be a novel approach to treating ischemic heart diseases.

Experimental Section

Chemical Methods. All commercial chemicals and solvents were reagent grade and used without further purification unless otherwise specified. The following solvents and reagents have been abbreviated: dichloromethane (DCM), tetrahydrofuran (THF), dimethyl sulfoxide (DMSO), chloroform ($CHCl_3$), and dimethylformamide (DMF). All reactions except those in aqueous media were carried out under an argon atmosphere or with the use of standard techniques for the exclusion of moisture. Reactions were monitored by thin-layer chromatography on 0.25 mm silica gel plates (Merck Kieselgel 60 and 60 F_{254}) and visualized with UV light, iodine vapors, or 5% phosphomolybdic acid in EtOH. Standard workup procedures were used for all the reactions, and solvents were dried over $MgSO_4$ before evaporation. The final compounds were typically purified either by TLC on silica gel or by reversed-phase HPLC.

Analytical purity was assessed by RP-HPLC using a Varian Polaris C18-A column (0.46 mm × 100 mm) equipped with a diode array spectrometer. The mobile phase employed 0.1% formic acid or 0.1% trifluoroacetic acid with acetonitrile at a flow rate of 2.0 mL/min.

^1H and ^{13}C NMR data were recorded on a Varian Unity-400 Plus instrument. Chemical shifts were reported in parts per million (ppm) and autocalibrated to the deuterated solvent reference peaks. Coupling constants were reported in units of hertz (Hz). Mass spectra were acquired in either the positive or negative ion mode under electrospray ionization (ESI) on a Finnigan LCQ Iontrap mass spectrometer.

In Vitro MCD Inhibitory Activity Assay. The decarboxylase activity of MCD was measured spectrophotometrically by monitoring acetyl-CoA formation using the malate dehydrogenase (MD)/citrate synthase (CS) coupling system. The conversion of acetyl-CoA from malonyl-CoA was assayed using a modified protocol as previously described by Kim and Kolattukudy.[24] The establishment of the kinetic equilibrium between malate/NAD and oxaloacetate/NADH was catalyzed by malate dehydrogenase. The enzymatic reaction product of MCD, acetyl-CoA, shifted the equilibrium by condensing with oxaloacetate in the presence of citrate synthase, which resulted in a continuous generation of NADH from NAD. The accumulation of NADH was continuously followed by monitoring the increase of fluorescence emission at 465 nm on a fluorescence plate reader. The fluorescence plate reader was calibrated using authentic acetyl-CoA from Sigma. For a typical 96-well plate assay, the increase in the fluorescence emission (λ_{ex} = 340 nm and λ_{em} = 465 nm for NADH) in each well was used to calculate the initial velocity of human recombinant MCD. Each 50 μL assay contained 10 mM phosphate buffered saline (Sigma), pH 7.4, 0.05% Tween-20, 25 mM $K_2HPO_4-KH_2PO_4$ (Sigma), 2 mM malate (Sigma), 2 mM NAD (Boehringer Mannheim), 0.786 units of MD (Roche Chemicals), 0.028 unit of CS (Roche Chemicals), 5−10 nM hMCD, and varying amounts of MCA substrate. Assays were initiated by the addition of MCA, and the rates were corrected for the background rate determined in the absence of hMCD.

Isolated Working Rat Heart Assay. Isolated working hearts from male Sprague-Dawley rats (300−350 g) are subjected to a

60-min aerobic perfusion period.[11] The working hearts were perfused (95% O_2 and 5% CO_2) with a modified Krebs−Henseleit solution containing 5 mM glucose, 100 μU/mL insulin, 3% fatty acid-free BSA, 2.5 mM free Ca^{2+}, and 0.4−1.2 mM palmitate. The test compound was added 5 min before the perfusion period. DMSO (0.05%) is used as a control.

Measurement of Glucose Oxidation Rates. Samples were taken at 10-min intervals throughout the 60-min perfusion for measurements of glucose oxidation. Glucose oxidation rates were determined by the quantitative collection of $^{14}CO_2$ produced by hearts perfused with buffer containing [U-^{14}C]glucose. Gaseous $^{14}CO_2$ was trapped in hyamine hydroxide and sampled at 10-min intervals. After the perfusion, the $^{14}CO_2$ from the perfusate was subsequently released by injecting 1 mL of perfusate into a sealed test tube containing 1 mL of 9 N H_2SO_4. The tube was sealed with a rubber stopper attached to a scintillation vial containing a piece of filter paper saturated with 300 μL of hyamine hydroxide. The scintillation vials with filter papers were then removed, and Ecolite scintillation fluid was added. Samples were counted by standard procedures as described above. Average rates of glucose oxidation for each phase of perfusion are expressed as nmol/min per gram of dry weight.

General Synthesis of Amide Compounds 5. 2-(*p*-*N*-Alkylphenyl)hexafluoroisopropanol (0.6 mmol) and poly(4-vinylpyridine) (204.5 mg, 1.8 mmol) are mixed in CH_2Cl_2 (3 mL). Acyl chloride (0.6 mmol) is added to the suspension, and the reaction mixture is stirred at room temperature overnight. The polymer is removed by filtration through a pad of Celite, and the organic solvent is removed under reduced pressure. The residue is purified by preparative TLC (hexane/EtOAc, 7:3) to afford the desired compound.

2-Phenoxy-*N*-[4-(2,2,2-trifluoro-1-hydroxy-1-trifluoromethylethyl)phenyl]acetamide (5a). ^{1}H NMR (DMSO-d_6) δ 4.7 (s. 2H), 6.96 (m, 3H), 7.28 (t, 2H), 7.6 (d, 2H), 7.74 (d, 2H); ESIMS *m*/*z* 394 (M + H).

3-Phenyl-*N*-[4-(2,2,2-trifluoro-1-hydroxy-1-trifluoromethylethyl)phenyl]propionamide (5b). ^{1}H NMR (DMSO-d_6) δ 2.62 (t, 2H), 2.88 (t, 2H), 7.15 (m, 2H), 7.25 (m, 3H), 7.55 (d, 2H), 7.66 (d, 2H); ES/MS *m*/*z* 392 (M + H).

***N*-Methyl-3-phenyl-*N*-[4-(2,2,2-trifluoro-1-hydroxy-1-trifluoromethylethyl)phenyl]propionamide (5c).** ^{1}H NMR ($CDCl_3$) δ 2.68 (t, 2H), 3.03 (t, 2H), 3.21 (s, 3H), 7.01 (m,2H), 7.25 (m, 3H), 7.66 (d, 2H), 7.76 (d, 2H); ESIMS *m*/*z* 406 (M + H).

***N*-Ethyl-3-phenyl-*N*-[4-(2,2,2-trifluoro-1-hydroxy-1-trifluoromethylethyl)phenyl]propionamide (5d).** ^{1}H NMR ($CDCl_3$) δ 1.02 (t, 3H), 2.3 (t, 2H), 2.82 (t, 1H), 6.98 (m, 4H), 7.20 (m, 3H), 7.82 (d, 2H); ESIMS *m*/*z* 420 (M + H).

***N*-Isopropyl-3-phenyl-*N*-[4-(2,2,2-trifluoro-1-hydroxy-1-trifluoromethylethyl)phenyl]propionamide (5e).** ^{1}H NMR ($CDCl_3$) δ 1.00 (d, 6H), 2.2 (t, 3H), 2.81 (t, 2H), 4.98 (m, 1H), 6.88 (d, 2H), 6.95 (d, 2H), 7.19 (m, 3H), 7.78 (d, 2H); ESIMS *m*/*z* 434.2-(M + H).

***N*-Butyl-3-phenyl-*N*-[4-(2,2,2-trifluoro-1-hydroxy-1-trifluoromethylethyl)phenyl]propionamide (5f).** ^{1}H NMR ($CDCl_3$) δ 0.82 (t, 3H), 1.23 (m, 2H), 1.4 (m, 2H), 2.3 (t, 2H), 2.8 (t, 2H), 3.61 (t, 2H), 6.98 (d, 2H), 7.02 (d, 2H), 7.2 (m, 3H), 7.7 (d, 2H); ESIMS *m*/*z* 448 (M + H).

{(3-Phenylpropionyl)-[4-(2,2,2-trifluoro-1-hydroxy-1-trifluoromethylethyl)phenyl]amino}acetic Acid Methyl Ester (5g). ^{1}H NMR ($CDCl_3$) δ 2.42 (t, 2H), 2.84(t, 2H), 3.71 (s, 3H), 4.3 (s, 2H), 7.0 (d, 2H), 7.2 (m, 3H), 7.26 (d, 2H), 7.76 (d, 2H); ESIMS *m*/*z* 464 (M + H).

{(3-Phenylpropionyl)-[4-(2,2,2-trifluoro-1-hydroxy-1-trifluoromethylethyl)phenyl]amino}acetic Acid (5h). ^{1}H NMR ($CDCl_3$) δ 2.42 (t, 2H), 2.84 (t, 2H), 4.32 (s, 2H), 7.0 (d, 2H), 7.18 (m, 3H), 7.22 (d, 2H), 7.76 (d, 2H); ESIMS *m*/*z* 450 (M + H).

***N*-Benzyl-3-phenyl-*N*-[4-(2,2,2-trifluoro-1-hydroxy-1-trifluoromethylethyl)phenyl]propionamide (5i).** ^{1}H NMR ($CDCl_3$) δ 2.37 (t, 2H), 2.91 (t, 2H), 4.80 (s, 2H), 6.80 (d, 2H), 7.01 (d, 2H), 7.08 (m, 2H), 7.18 (d, 2H), 7.23 (m, 4H), 7.68 (d, 2H); ESIMS *m*/*z* 482 (M + H).

***N*-Cyclohexyl-3-phenyl-*N*-[4-(2,2,2-trifluoro-1-hydroxy-1-trifluoromethylethyl)phenyl]propionamide (5j).** ^{1}H NMR ($CDCl_3$) δ 0.95 (m, 3H), 1.32 (m, 2H), 1.52 (d, 1H), 1.70 (t, 4H), 2.15 (t, 2H), 2.81 (t, 2H), 4.58 (m, 1H), 6.85 (d, 2H), 6.93 (d, 2H), 7.18 (m, 3H), 7.75 (d, 2H); ESIMS *m*/*z* 474 (M + H).

***N*-[4-(2,2,2-Trifluoro-1-hydroxy-1-trifluoromethylethyl)phenyl]isobutyramide (5k).** ^{1}H NMR (DMSO) δ 1.07 (d, 6H), 2.57 (m, 1H), 7.55 (d, 2H), 7.70 (d, 2H), 8.52 (s, 1H), 10.0 (s, 1H); ESIMS *m*/*z* 330.1 (M + H).

***N*-Methyl-*N*-[4-(2,2,2-trifluoro-1-hydroxy-1-trifluoromethylethyl)phenyl]isobutyramide (5l).** ^{1}H NMR (CD_3OD) δ 1.07 (d, 6H), 2.52 (m, 1H), 3.21 (s, 3H), 7.40 (d, 2H), 7.82 (d, 2H); ESIMS *m*/*z* 344 (M + H).

***N*-Methyl-*N*-[4-(2,2,2-trifluoro-1-hydroxy-1-trifluoromethylethyl)phenyl]nicotinamide (5m).** ^{1}H NMR (CD_3OD) δ 3.5 (s, 3H), 7.3 (m,3H), 7.6 (d, 2H), 7.7 (d, 1H), 8.4 (m, 2H); ESIMS *m*/*z* 379 (M + H).

***N*-Methyl-*N*-[4-(2,2,2-trifluoro-1-hydroxy-1-trifluoromethylethyl)phenyl]isonicotinamide (5n).** ^{1}H NMR (CD_3OD) δ 3.45 (s, 3H), 7.30 (m, 4H), 7.62 (d, 2H), 8.41 (d, 2H); ESIMS *m*/*z* 379 (M + H).

***N*-Ethyl-*N*-[4-(2,2,2-trifluoro-1-hydroxy-1-trifluoromethylethyl)phenyl]isobutyramide (5o).** ^{1}H NMR ($CDCl_3$) δ 1.0 (d, 6H), 1.2 (t, 3H), 2.4 (m, 1H), 3.7 (q, 2H), 738 (d, 2H), 7.82 (d, 2H); ESIMS *m*/*z* 358 (M + H).

***N*-Propyl-*N*-[4-(2,2,2-trifluoro-1-hydroxy-1-trifluoromethylethyl)phenyl]isobutyramide (5p).** ^{1}H NMR ($CDCl_3$) δ 0.82 (t, 3H), 1.0 (d, 6H), 1.5 (m, 2H), 2.4 (m, 1H), 3.6 (t, 2H), 7.20 (d, 2H), 7.80 (d, 2H); ESIMS *m*/*z* 372 (M + H).

***N*-Butyl-*N*-[4-(2,2,2-trifluoro-1-hydroxy-1-trifluoromethylethyl)phenyl]isobutyramide (5q).** ^{1}H NMR ($CDCl_3$) δ 0.82 (t, 3H), 1.0 (d, 6H), 1.3 (m, 2H), 1.45 (m, 2H), 2.4 (m, 1H), 3.7 (t, 2H), 7.38 (d, 2H), 7.82 (d, 2H); ESIMS *m*/*z* 386 (M + H).

***N*-(2-Dimethylaminoethyl)-*N*-[4-(2,2,2-trifluoro-1-hydroxy-1-trifluoromethylethyl)phenyl]isobutyramide (5r).** ^{1}H NMR (CD_3OD) δ 1.2 (d, 6H), 2.31 (s, 6H), 2.61 (m, 1H), 2.72 (t, 2H), 3.68 (t, 2H), 7.52 (d, 2H), 7.76 (d, 2H); ESIMS *m*/*z* 401(M + H).

***N*-(2-Hydroxyethyl)-*N*-[4-(2,2,2-trifluoro-1-hydroxy-1-trifluoromethylethyl)phenyl]isobutyramide (5s).** ^{1}H NMR ($CDCl_3$) δ 1.0 (d, 6H), 2.42 (m, 1H), 3.62 (t, 2H), 3.8 (t, 2H), 7.42 (d, 2H), 7.82 (d, 2H); ESIMS *m*/*z* 372 (M − H).

{Isobutyryl-[4-(2,2,2-trifluoro-1-hydroxy-1-trifluoromethylethyl)phenyl]amino}acetic Acid Methyl Ester (5t). ^{1}H NMR ($CDCl_3$) δ 1.02 (d, 6H), 2.52 (m, 1H), 3.72 (s, 3H), 4.32 (s, 2H), 7.42 (d, 2H), 7.8 (d, 2H); ESIMS *m*/*z* 400 (M − H).

{Isobutyryl-[4-(2,2,2-trifluoro-1-hydroxy-1-trifluoromethylethyl)phenyl]amino}acetic Acid (5u). ^{1}H NMR ($CDCl_3$) δ 1.02 (d, 6H), 2.58 (m, 1H), 4.32 (s, 2H), 7.45 (d, 2H), 7.8 (d, 2H); ESIMS *m*/*z* 386 (M − H).

5-{Isobutyryl-[4-(2,2,2-trifluoro-1-hydroxy-1-trifluoromethylethyl)phenyl]amino}pentanoic Acid Methyl Ester (5v). ^{1}H NMR ($CDCl_3$) δ 1.0 (d, 6H), 1.5 (m, 2H), 1.6 (m, 2H), 2.31 (t, 2H), 2.4 (m, 1H), 3.6 (s, 3H), 3.7 (t, 2H), 7.45 (d, 2H), 7.82 (d, 2H); ESIMS *m*/*z* 442 (M − H).

5-{Isobutyryl-[4-(2,2,2-trifluoro-1-hydroxy-1-trifluoromethylethyl)phenyl]amino}pentanoic Acid (5w). ^{1}H NMR ($CDCl_3$) δ 1.0 (d, 6H), 1.58 (m, 4H), 2.31 (t, 2H), 2.4 (m, 1H), 3.7 (t, 2H), 7.40 (d, 2H), 7.82 (d, 2H); ESIMS *m*/*z* 428 (M − H).

***N*-[4-(1*H*-Tetrazol-5-yl)butyl]-*N*-[4-(2,2,2-trifluoro-1-hydroxy-1-trifluoromethylethyl)phenyl]isobutyramide (5x).** ^{1}H NMR ($CDCl_3$) δ 1.0 (d, 6H), 1.52 (m, 2H), 1.78 (m, 2H), 2.4 (m, 1H), 2.91 (t, 2H), 3.72 (t, 2H), 7.38 (d, 2H), 7.82 (d, 2H); ESIMS *m*/*z* 452 (M − H).

***N*-(4-Cyanobutyl)-*N*-[4-(2,2,2-trifluoro-1-hydroxy-1-trifluoromethylethyl)phenyl]isobutyramide (5y).** ^{1}H NMR ($CDCl_3$) δ 1.0 (d, 6H), 1.62 (m, 4H), 2.42 (m, 3H), 3.72 (t, 2H), 7.40 (d, 2H), 7.82 (d, 2H); ESIMS *m*/*z* 409 (M − H).

4-Cyano-*N*-ethyl-*N*-[4-(2,2,2-trifluoro-1-hydroxy-1-trifluoromethylethyl)phenyl]benzamide (5z). ^{1}H NMR ($CDCl_3$) δ 1.20 (s, 3H), 3.71 (q, 2H); ESIMS *m*/*z* 417 (M + H).

***N*-Ethyl-*N*-[4-(2,2,2-trifluoro-1-hydroxy-1-trifluoromethylethyl)phenyl]isonicotinamide (5aa).** ^{1}H NMR (CD_3OD) δ 1.20 (s,

3H), 3.71 (q, 2H), 7.30 (m. 4H), 7.62 (d, 2H), 8.40 (d, 2H); ESIMS *m*/*z* 393 (M + H).

1-Phenyl-3-[4-(2,2,2-trifluoro-1-hydroxy-1-trifluoromethylethyl)phenyl]urea (6a). ^{1}H NMR (CD_3OD) δ 7.02 (t, 1H), 7.29 (t, 2H), 7.42 (d, 2H), 7.53 (d, 2H), 7.63 (d, 2H); ESIMS *m*/*z* 379 (M + H).

1-Methyl-3-phenyl-1-[4-(2,2,2-trifluoro-1-hydroxy-1-trifluoromethylethyl)phenyl]urea (6b). ^{1}H NMR (CD_3OD) δ 2.60 (s, 3H), 6.95 (t, 1H), 7.4 (m, 4H), 7.72 (d, 2H), 7.56 (d, 2H); ESIMS *m*/*z* 393 (M + H).

Morpholine-4-carboxylic Acid [4-(2,2,2-Trifluoro-1-hydroxy-1-trifluoromethylethyl)phenyl]amide (6c). ^{1}H NMR (CD_3OD) δ 3.35 (t, 4H), 3.56 (t, 4H), 7.28 (d, 2H), 7.48 (d, 2H); ^{13}C NMR (CD_3OD) δ 45.1, 67.4, 115.6, 119.6, 120.9, 122.6, 125.3, 126.3, 128.2, 141.6, 156.9; ESIMS *m*/*z* 371 (M − H).

1-Ethyl-3,3-dimethyl-1-[4-(2,2,2-trifluoro-1-hydroxy-1-trifluoromethylethyl)phenyl]urea (6d). ^{1}H NMR (CD_3OD) δ 1.13 (t, 3H), 2.70 (s, 6H), 3.20 (q, 2H), 7.17 (d, 2H), 7.57 (d, 2H); ESIMS *m*/*z* 359 (M + H).

1,3-Diethyl-3-(4-hydroxybutyl)-1-[4-(2,2,2-trifluoro-1-hydroxy-1-trifluoromethylethyl)phenyl]urea (6e). ^{1}H NMR (CD_3OD) δ 1.13 (t, 3H), 1.26 (t, 3H), 1.48 (m, 2H), 1.55 (m, 2H), 3.10−3.25 (m, 6H), 3.50 (t, 2H), 7.15 (d, 2H), 7.60 (d, 2H); ESIMS *m*/*z* 431 (M + H).

Morpholine-4-carboxylic Acid Methyl-[4-(2,2,2-trifluoro-1-hydroxy-1-trifluoromethylethyl)phenyl]amide (6f). ^{1}H NMR (CD_3OD) δ 2.78 (t, 3H), 3.18 (t, 4H), 3.42 (t, 4H), 7.12 (d, 2H), 7.64 (d, 2H); ESIMS *m*/*z* 387 (M + H).

Morpholine-4-carboxylic Acid Ethyl-[4-(2,2,2-trifluoro-1-hydroxy-1-trifluoromethylethyl)phenyl]amide (6g). ^{1}H NMR ($CDCl_3$) δ 1.12 (t, 3H), 3.18 (t, 4H), 3.42 (t, 4H), 3.65 (q, 2H), 7.12 (d, 2H), 7.64 (d, 2H); ESIMS *m*/*z* 401(M + H).

Morpholine-4-carboxylic Acid Propyl-[4-(2,2,2-trifluoro-1-hydroxy-1-trifluoromethylethyl)phenyl]amide (6h). ^{1}H NMR ($CDCl_3$) δ 0.82 (t, 3H), 1.60 (m, 2H), 3.18 (t, 4H), 3.42 (t, 4H), 3.61 (t, 2H), 7.12 (d, 2H), 7.64 (d, 2H); ESIMS *m*/*z* 413 (M − H).

Morpholine-4-carboxylic Acid Butyl-[4-(2,2,2-trifluoro-1-hydroxy-1-trifluoromethylethyl)phenyl]amide (6i). ^{1}H NMR (CD_3OD) δ 0.82 (t, 3H), 1.30 (m, 2H), 1.57 (m, 2H), 3.18 (t, 4H), 3.42 (t, 4H), 3.61 (t, 2H), 7.1 (d, 2H), 7.64 (d, 2H); ES/MS *m*/*z* 427 (M − H).

Morpholine-4-carboxylic Acid Pentyl-[4-(2,2,2-trifluoro-1-hydroxy-1-trifluoromethylethyl)phenyl]amide (6j). ^{1}H NMR ($CDCl_3$) δ 0.82 (t, 3H), 1.25 (m. 4H), 1.59 (m, 2H), 3.18 (t, 4H), 3.42 (t, 4H), 3.61 (t, 2H), 7.10 (d, 2H), 7.53 (d, 2H); ^{13}C NMR ($CDCl_3$) δ 15.1, 23.4, 29.4, 30.3, 47.1, 52.7, 67.3, 122.3, 124.6, 125.3, 126.6, 128.1, 129.1, 148.1, 161.3; ESIMS *m*/*z* 443 (M + H).

Morpholine-4-carboxylic Acid Hexyl-[4-(2,2,2-trifluoro-1-hydroxy-1-trifluoromethylethyl)phenyl]amide (6k). ^{1}H NMR ($CDCl_3$) δ 0.82 (t, 3H), 1.25 (m, 6H), 1.59 (m, 2H), 3.18 (t, 4H), 3.42 (t, 4H), 3.61 (t, 2H), 7.12 (d, 2H), 7.64 (d, 2H); ^{13}C NMR ($CDCl_3$) δ 14.6, 23.4, 27.6, 29.6, 32.3, 46.9, 52.6, 67.1, 119.4, 122.1, 124.1, 124.9, 126.4, 128.9, 148.0, 160.6; ESIMS *m*/*z* 457 (M + H).

Morpholine-4-carboxylic Acid Heptyl-[4-(2,2,2-trifluoro-1-hydroxy-1-trifluoromethylethyl)phenyl]amide (6l). ^{1}H NMR ($CDCl_3$) δ 0.82 (t, 3H), 1.25 (m, 8H), 1.59 (m, 2H), 3.18 (t, 4H), 3.42 (t, 4H), 3.61 (t, 2H), 7.12 (d, 2H), 7.64 (d, 2H); ^{13}C NMR ($CDCl_3$) δ 14.9, 23.4, 28.0, 29.9, 30.0, 32.7, 47.0, 52.7, 67.1, 119.4, 122.3, 124.3, 125.1, 126.4, 128.0, 129.0, 148.0, 161.1; ESIMS *m*/*z* 471 (M + H).

Morpholine-4-carboxylic Acid Octyl-[4-(2,2,2-trifluoro-1-hydroxy-1-trifluoromethylethyl)phenyl]amide (6m). ^{1}H NMR (CD_3OD) δ 0.82 (t, 3H), 1.25 (m, 10H), 1.59 (m, 2H), 3.18 (t, 4H), 3.42 (t, 4H), 3.61 (t, 2H), 7.12 (d, 2H), 7.64 (d, 2H); ^{13}C NMR ($CDCl_3$) δ 14.9, 23.6, 28.0, 29.7, 30.2, 30.3, 32.7, 47.0, 52.7, 67.1, 116.9, 122.1, 124.3, 125.0, 126.1, 128.9, 148.0, 161.0; ESIMS *m*/*z* 483(M − H).

Morpholine-4-carboxylic Acid Phenethyl-[4-(2,2,2-trifluoro-1-hydroxy-1-trifluoromethylethyl)phenyl]amide (6n). ^{1}H NMR ($CDCl_3$) δ 2.90 (t, 2H), 3.18 (t, 4H), 3.42 (t, 4H), 3.81 (t, 2H), 6.91 (d, 2H), 7.18 (m, 3H), 7.23 (d, 2H), 7.64 (d, 2H); ^{13}C NMR ($CDCl_3$) δ 35.9, 46.9, 54.9, 67.1, 119.4, 122.3, 123.9, 124.6, 125.0, 125.3, 126.4, 127.4, 128.9, 129.4, 130.0, 140.3, 148.3, 160.9; ESIMS *m*/*z* 475 (M − H).

Morpholine-4-carboxylic Acid (2-Hydroxyethyl)-[4-(2,2,2-trifluoro-1-hydroxy-1-trifluoromethylethyl)phenyl]amide (6o). ^{1}H NMR ($CDCl_3$) δ 3.18 (t, 4H), 3.42 (t, 4H), 3.6 (t, 2H), 3.82 (t, 2H), 7.18 (d, 2H), 7.72 (d, 2H); ESIMS *m*/*z* 415 (M − H).

{(Morpholine-4-carbonyl)-[4-(2,2,2-trifluoro-1-hydroxy-1-trifluoromethylethyl)phenyl]amino}acetic Acid Methyl Ester (6p). ^{1}H NMR (CD_3OD) δ 3.18 (t, 4H), 3.42 (t, 4H), 3.68 (s, 3H), 4.38 (s, 2H), 7.1 (d, 2H), 7.64 (d, 2H); ESIMS *m*/*z* 443 (M − H).

3-{(Morpholine-4-carbonyl)-[4-(2,2,2-trifluoro-1-hydroxy-1-trifluoromethylethyl)phenyl]amino}propionic Acid Methyl Ester (6q). ^{1}H NMR ($CDCl_3$) δ 2.62 (t, 2H), 3.18 (t, 4H), 3.42 (t, 4H), 3.58 (s, 3H), 3.91 (t, 2H), 7.05 (d, 2H), 7.62 (d, 2H); ESIMS *m*/*z* 457 (M − H).

3-{(Morpholine-4-carbonyl)-[4-(2,2,2-trifluoro-1-hydroxy-1-trifluoromethylethyl)phenyl]amino}propionic Acid (6r). ^{1}H NMR ($CDCl_3$) δ 2.52 (t, 2H), 3.18 (t, 4H), 3.42 (t, 4H), 3.82 (t, 2H), 7.15 (d, 2H), 7.62 (d, 2H); ESIMS *m*/*z* 445 (M + H).

4-{(Morpholine-4-carbonyl)-[4-(2,2,2-trifluoro-1-hydroxy-1-trifluoromethylethyl)phenyl]amino}butyric Acid Methyl Ester (6s). ^{1}H NMR ($CDCl_3$) δ 0.82 (m, 2H), 2.32 (t, 2H), 3.18 (t, 4H), 3.42 (t, 4H), 3.58 (s, 3H), 3.62 (t, 2H), 7.05 (d, 2H), 7.62 (d, 2H); ESIMS *m*/*z* 471 (M − H).

Morpholine-4-carboxylic Acid (3-Cyanopropyl)-[4-(2,2,2-trifluoro-1-hydroxy-1-trifluoromethylethyl)phenyl]amide (6t). ^{1}H NMR (CD_3OD) δ 1.92 (m, 2H), 2.40 (t, 2H), 3.18 (t, 4H), 3.42 (t, 4H), 3.74 (t, 2H), 7.15 (d, 2H), 7.72 (d, 2H); ^{13}C NMR (CD_3OD) δ 15.7, 24.9, 46.7, 50.9, 67.0, 119.4, 120.1, 122.1, 124.9, 125.0, 127.9, 128.0, 129.7, 146.9, 161.0; ESIMS *m*/*z* 438 (M − H).

5-{(Morpholine-4-carbonyl)-[4-(2,2,2-trifluoro-1-hydroxy-1-trifluoromethylethyl)phenyl]amino}pentanoic Acid Methyl Ester (6u). ^{1}H NMR ($CDCl_3$) δ 1.60 (m, 4H), 2.31 (t, 2H), 3.15 (t, 4H), 3.42 (t, 4H), 3.6 (s, 3H), 3.61 (t, 2H), 7.08 (d, 2H), 7.64 (d, 2H); ^{13}C NMR ($CDCl_3$) δ 23.3, 29.0, 32.7, 47.0, 52.1, 52.4, 67.1, 119.4, 123.3, 124.6, 125.1, 127.1, 128.0, 129.1, 147.6, 161.1, 174.9; ESIMS *m*/*z* 485 (M − H).

5-{(Morpholine-4-carbonyl)-[4-(2,2,2-trifluoro-1-hydroxy-1-trifluoromethylethyl)phenyl]amino}pentanoic Acid (6v). ^{1}H NMR ($CDCl_3$) δ 1.59 (m, 4H), 2.28 (m, 2H), 3.15 (t, 4H), 3.42 (t, 4H), 3.61 (t, 2H), 7.08 (d, 2H), 7.64 (d, 2H); ^{13}C NMR ($CDCl_3$) δ 23.4, 29.1, 32.7, 46.9, 52.2, 67.0, 119.4, 123.3, 124.6, 125.1, 127.1, 128.0, 129.1, 147.4, 161.0, 172.1; ESIMS *m*/*z* 471 (M − H).

***N*-Methyl-2-phenoxy-*N*-[3-(2,2,2-trifluoro-1-hydroxy-1-trifluoromethylethyl)phenyl]acetamide (9).** A mixture of 2-(3-aminophenyl)-1,1,1,3,3,3-hexafluoropropan-2-ol (210 mg, 0.81 mmol) and triethylamine (160 μL, 0.89 mmol) in 3 mL of anhydrous dichloromethane was added dropwise to a solution of phenoxyacetyl chloride (145 mg, 0.85 mmol) in 3 mL of anhydrous dichloromethane. The light-yellow solution was then stirred at room temperature overnight. The reaction mixture was then washed with water and then brine. After drying over magnesium sulfate, the organic phase was concentrated in vacuo. The resulting white solid was purified by preparative TLC (5% methanol, 95% chloroform) to yield 260 mg (81.8%). ^{1}H NMR ($CDCl_3$) δ 4.51 (s, 2H), 6.94 (d, 2H), 7.00 (t, J = 7.6 Hz, 1H), 7.28 (t, 2H), 7.36 (t, J = 8 Hz, 1H), 7.46 (d, J = 7.6 Hz, 1H), 7.67 (d, 1H), 7.85 (s, 1H); ESIMS *m*/*z* 394 (M + H).

Sodium hydride (30 mg, 0.693 mmol) was suspended in dry THF under an argon atmosphere. 2-Phenoxy-*N*-[3-(2,2,2-trifluoro-1-hydroxy-1-trifluoromethylethyl)phenyl]acetamide (181.7 mg, 0.462 mmol) was added at 0 °C. The reaction mixture was then stirred at room temperature for 45 min. Methyl iodide (45 μL, 0.693 mmol) was added, and the light-yellow solution was stirred at room temperature overnight. The reaction mixture was then diluted with diethyl ether. The organic layer was separated, washed with water and brine, and dried over magnesium sulfate. The solvent was concentrated in vacuo, and the resulting colorless oil was purified

by preparative TLC (5% methanol, 95% chloroform) to yield the title compound (150 mg). ^{1}H NMR ($CDCl_3$) δ 3.22 (s, 3H), 4.51 (s, 2H), 6.6 (d, J = 7.6 Hz, 2H), 6.83 (t, J = 7.2 Hz, 1H), 7.12 (t, J = 8 Hz, 2H), 7.26 (d, 1H), 7.44 (t, J = 8.4 Hz, 1H), 7.59 (s, 1H), 7.68 (d, J = 7.6 Hz, 1H); ESIMS *m*/*z* 408 (M + H).

***N*-Phenethyl-4-(2,2,2-trifluoro-1-hydroxy-1-trifluoromethylethyl)benzamide (11a).** ^{1}H NMR (CD_3OD) δ 2.90 (t, 2H), 3.59 (t, 2H), 7.22 (m, 5H), 7.81 (m, 4H); ESIMS *m*/*z* 392 (M + H).

***N*-Methyl-*N*-phenethyl-4-(2,2,2-trifluoro-1-hydroxy-1-trifluoromethylethyl)benzamide (11b).** ^{1}H NMR (CD_3OD) δ 2.77 (t, 2H), 2.98 (t, 1H), 3.10 (s, 3H), 3.47 (t, 1H), 3.75 (t, 1H), 6.88 (t, 1H), 7.02 (d, 1H), 7.18 (d, 2H), 7.30 (d, 2H), 7.38 (d, 1H), 7.66 (d, 1H), 7.79 (d, 1H); ESIMS *m*/*z* 406 (M + H).

***N*-Benzyl-*N*-methyl-4-(2,2,2-trifluoro-1-hydroxy-1-trifluoromethylethyl)benzamide (11c).** ^{1}H NMR (CD_3OD) δ 2.94 (s, 3H), 4.50 (s, 2H), 7.15 (m, 1H), 7.3 (m, 2H), 7.55 (m, 3H), 7.81 (m, 3H); ESIMS *m*/*z* 392 (M + H).

***N*-Methoxy-*N*-methyl-4-(2,2,2-trifluoro-1-hydroxy-1-trifluoromethylethyl)benzamide (11d).** ^{1}H NMR (CD_3OD) δ 3.37 (s, 3H), 3.52 (s, 3H), 7.71 (m, 4H); ESIMS *m*/*z* 332 (M + H).

Pyrrolidin-1-yl-[4-(2,2,2-trifluoro-1-hydroxy-1-trifluoromethylethyl)phenyl]methanone (11e). ^{1}H NMR (CD_3OD) δ 1.9 (m, 2H), 1.98 (m, 2H), 3.43 (t, 2H), 3.58 (t, 2H), 7.61 (d, 2H), 7.81 (d, 2H); ESIMS *m*/*z* 342 (M + H).

Morpholin-4-yl-[4-(2,2,2-trifluoro-1-hydroxy-1-trifluoromethylethyl)phenyl]methanone (11f). ^{1}H NMR (CD_3OD) δ 3.4−3.8 (m, 8H), 7.52 (d, 2H), 7.81 (d, 2H); ESIMS *m*/*z* 358 (M + H).

Piperidin-1-yl-[4-(2,2,2-trifluoro-1-hydroxy-1-trifluoromethylethyl)phenyl]methanone (11g). ^{1}H NMR (CD_3OD) δ 1.7 (m, 6H), 3.38 (m, 2H), 3.7 (m, 2H), 7.46 (d, 2H), 7.81 (d, 2H); ESIMS *m*/*z* 356 (M + H).

***N*-(2-Cyanoethyl)-*N*-ethyl-4-(2,2,2-trifluoro-1-hydroxy-1-trifluoromethylethyl)benzamide (11h).** ^{1}H NMR (CD_3OD) δ 1.15 (t, 3H), 2.88 (t, 2H), 3.38 (t, 2H), 3.78 (t, 2H), 7.46 (d, 2H), 7.81 (d, 2H); ESIMS *m*/*z* 369 (M + H).

***N*,*N*-Diisobutyl-4-(2,2,2-trifluoro-1-hydroxy-1-trifluoromethylethyl)benzamide (11i).** ^{1}H NMR (CD_3OD) δ 0.75 (d, 6H), 0.96 (d, 6H), 1.86 (m, 1H), 2.15 (m, 1H), 3.14 (d, 2H), 3.38 (d, 2H), 7.45 (d, 2H), 7.81 (d, 2H); ESIMS *m*/*z* 398 (M − H).

Acknowledgment. We thank Prof. William Stanley at Case Western Reserve University for helping with Figure 1. The authors also thank Dr. Peter Simms, Cynthia Jefferies, and Aixia Sun for their help with HPLC and MS analysis.

Supporting Information Available: HPLC and ^{1}H NMR data for listed compounds. This material is available free of charge via the Internet at http://pubs.acs.org.

References

(1) (a) Kim, Y. S.; Kolattukudy, P. E. Purification and Properties of Malonyl-CoA Decarboxylase from Rat Liver Mitochondria and Its Immunological Comparison with the Enzymes from Rat Brain, Heart, and Mammary Gland. *Arch. Biochem. Biophys.* **1978**, *190*, 234−246. (b) Kim, Y. S.; Kolattukudy, P. E. Malonyl-CoA Decarboxylase from the Uropygial Gland of Waterfowl: Purification, Properties, Immunological Comparison, and Role in Regulating the Synthesis of Multimethyl-Branched Fatty Acids. *Arch. Biochem. Biophys*. **1978**, *190*, 585−597. (c) Kim, Y. S.; Kolattukudy, P. E. Malonyl-CoA Decarboxylase from the Mammary Gland of Lactating Rat. Purification, Properties and Subcellular Localization. *Biochim. Biophys. Acta*. **1978**, *531*, 187−196. (d) Kim, Y. S.; Kolattukudy, P. E.; Boos, A. Malonyl-CoA Decarboxylase in Rat Brain Mitochondria. *Int. J. Biochem*. **1979**, *10*, 551−555. (e) Kim, Y. S.; Kolattukudy, P. E.; Boos, A. Malonyl-CoA Decarboxylase from *Mycobacterium tuberculosis* and *Pseudomonas fluorescens*. *Arch. Biochem. Biophys*. **1979**, *196*, 543−551. (f) Hunaiti, A. R.; Kolattukudy, P. E. Malonyl-CoA Decarboxylase from S*treptomyces Erythreus*: Purification, Properties, and Possible Role in the Production of Erythromycin. *Arch. Biochem. Biophys*. **1984**, *229*, 426−439. (g) Jang, S. H.; Cheesbrough, T. M.; Kolattukudy, P. E. Molecular Cloning, Nucleotide Sequence, and Tissue Distribution of Malonyl-CoA Decarboxylase. *J. Biol. Chem.* **1989**, *264*, 3500−3505. (h) Dyck, J. R.; Barr, A. J.; Barr, R. L.; Kolattukudy, P. E.; Lopaschuk, G. D. Characterization of Cardiac Malonyl-CoA Decarboxylase and Its Putative Role in Regulating Fatty Acid Oxidation. *Am. J. Physiol.* **1998**, *275* (6, Part 2), H2122−H2129.

(2) Gao, J.; Waber, L.; Bennett, M. J.; Gibson, K. M.; Cohen, J. C. Cloning and Mutational Analysis of Human Malonyl-coenzyme A Decarboxylase. *J. Lipid Res.* **1999**, *40*, 178. (b) Sacksteder, K. A.; Morrell, J. C.; Wanders, R. J.; Matalon, R.; Gould, S. J. MCD Encodes Peroxisomal and Cytoplasmic Forms of Malonyl-CoA Decarboxylase and Is Mutated in Malonyl-CoA Decarboxylase Deficiency. *J. Biol. Chem.* **1999**, *274*, 24461. (c) FitzPatrick, D. R.; Hill, A.; Tolmie, J. L.; Thorburn, D. R.; Christodoulou, J. The Molecular Basis of Malonyl-CoA Decarboxylase Deficiency. *Am. J. Hum. Genet.* **1999**, *65*, 318. (d) Surendran, S.; Sacksteder, K. A.; Gould, S. J.; Coldwell, J. G.; Rady, P. L.; Tyring, S. K.; Matalon, R. Malonyl CoA Decarboxylase Deficiency: C to T Transition in Intron 2 of the MCD Gene. *J. Neurosci. Res*. **2001**, *65*, 591−594.

(3) (a) Alam, N.; Saggerson, E. D. Malonyl-CoA and the Regulation of Fatty Acid Oxidation in Soleus Muscle. *Biochem. J*. **1998**, *334*, 233−241. (b) Sambandam, N.; Steinmetz, M.; Chu, A.; Altarejos, J. Y.; Dyck, J. R.; Lopaschuk, G. D. Malonyl-CoA Decarboxylase (MCD) Is Differentially Regulated in Subcellular Compartments by 5′AMP-Activated Protein Kinase (AMPK). Studies Using H9c2 Cells Overexpressing MCD and AMPK by Adenoviral Gene Transfer Technique. *Eur. J. Biochem.* **2004**, *271*, 2831−2840.

(4) Jolya, E.; Bendayan, M.; Roduita, R.; Saha, A. K.; Rudermand, N. B.; Prentki, M. Malonyl-CoA Decarboxylase Is Present in the Cytosolic, Mitochondrial and Peroxisomal Compartments of Rat Hepatocytes. *FEBS Lett.* **2005**, *579*, 6581−6586.

(5) Zammit, V. A. The Malonyl-CoA-Long-Chain Acyl-CoA Axis in the Maintenance of Mammalian Cell Function. *Biochem. J*. **1999**, *343*, 505−515.

(6) McGarry, J. D.; Brown, N. F. The Mitochondrial Carnitine Palmitoyltransferase System. From Concept to Molecular Analysis. *Eur. J. Biochem*. **1997**, *244*, 1−14.

(7) (a) Randle, P. J. Garland, P. B.; Hales, C. N.; Newsholme, E. A. The Glucose−Fatty Acid Cycle. Its Role in Insulin Sensitivity and the Metabolic Disturbances of Diabetes Mellitus. *Lancet* **1963**, *1*, 785−789. (b) Randle, P. J. Regulatory Interactions between Lipids and Carbohydrates: The Glucose Fatty Acid Cycle after 35 Years. *Diabetes Metab Rev.* **1998,** *14* (4), 263−283.

(8) Hearse, D. *Metabolic Approaches to Ischemic Heart Disease and Its Management*; Science Press Ltd.: New York, 1998.

(9) Kennedy, J. A.; Unger, S. A.; Horowitz, J. D. Inhibition of Carnitine Palmitoyltransferase-1 in Rat Heart and Liver by Perhexiline and Amiodarone. *Biochem. Pharmacol.* **1996**, *52*, 273−280.

(10) (a) McCormack, J. G.; Barr, R. L.; Wolff, A. A.; Lopaschuk, G. D. Ranolazine Stimulates Glucose Oxidation in Normoxic, Ischemic, and Reperfused Ischemic Rat Hearts. *Circulation* **1996**, *93*, 135−142. (b) McCormack, J. G.; Stanley, W. C.; Wolff, A. A. Ranolazine: A Novel Metabolic Modulator for the Treatment of Angina. *Genet. Pharmacol.* **1998**, *30*, 639−645. (c) Pepine, C. J.; Wolff, A. A. A Controlled Trial with a Novel Anti-Ischemic Agent, Ranolazine, in Chronic Stable Angina Pectoris That Is Responsive to Conventional Antianginal Agents. Ranolazine Study Group. *Am. J. Cardiol.* **1999**, *84*, 46−50.

(11) Kantor, P. F.; Lucien, A.; Kozak, R.; Lopaschuk, G. D. The Antianginal Drug Trimetazidine Shifts Cardiac Energy Metabolism from Fatty Acid Oxidation to Glucose Oxidation by Inhibiting Mitochondrial Long-Chain 3-Ketoacyl Coenzyme A Thiolase. *Circ. Res*. **2000**, *86*, 580−588.

(12) Dyck, J. D.; Cheng, J.-F.; Stanley, W.; Barr, R.; Chandler, M. P.; Brown, S.; Wallace, D.; Arrhenius, T.; Harmon, C.; Yang, G.; Nadzan, A.; Lopsaschuk, G. D. Malonyl-CoA Decarboxylase Inhibition Protects the Ischemic Heart by Inhibiting Fatty Acid Oxidation and Stimulating Glucose Oxidation. *Circ. Res.* **2004**, *94*, e78−e84.

(13) (a) Anderson, R. C. Carnitine Palmitoyltransferase: A Viable Target for the Treatment of NIDDM? *Curr. Pharm. Des.* **1998**, *4*, 1−16. (b) Deems, R. O.; Anderson, R. C.; Foley, J. E. Hypoglycemic Effects of a Novel Fatty Acid Oxidation Inhibitor in Rats and Monkeys. *Am. J. Physiol.* **1998**, *274*, R524−R528.

(14) Oh, W.; Abu-Elheiga, L.; Kordari, P.; Gu, Z.; Shaikenov, T.; Chirala, S. S.; Wakil, S. J. Glucose and Fat Metabolism in Adipose Tissue of Acetyl-CoA Carboxylase 2 Knockout Mice. *Proc. Natl. Acad. Sci. U.S.A.* **2005**, *102*, 1384−1389.

(15) An, J.; Muoio, D. M.; Shiota, M.; Fujimoto, Y.; Cline, G. W.; Shulman, G. I.; Koves, T. R.; Stevens, R.; Millington, D.; Newgard, C. B. Hepatic Expression of Malonyl-CoA Decarboxylase Reverses Muscle, Liver and Whole-Animal Insulin Resistance. *Nat. Med.* **2004**, *10*, 268−274.

(16) Zhou, D.; Yuen, P.; Chu, D.; Thon, V.; McConnell, S.; Brown, S.; Tsang, A.; Pena, M.; Russell, A.; Cheng, J.-F.; Barbosa, M.; Nadzan, A. M.; Yang, G.; Dyck, J. R. B.; Lopaschuk, G. D. Expression, Purification and Characterization of Human Malonyl-CoA Decarboxylase. *Protein Expression Purif.* **2004**, *34* (2), 261−269.
(17) Tularik group reported similar hexafluoroisopropanol-containing compounds as LXR agonists. Li, L.; Medina, J. C.; Hasegawa, H.; Cutler, S.; Liu, J.; Zhu, L.; Shan, B.; Lustig, K. LXR Modulator. World Patent WO 00/54759, 2000.
(18) Chkanikov, N. D.; Sviridov, V. D.; Zelenin, A. E.; Galakhov, M. V.; Kolomiets, A. F.; Fokin, A. V. *Bull. Acad. Sci. USSR, Div. Chem. Sci. (Engl. Transl.)* **1990**, *39*, 323−328.
(19) Sheppard, W. A. The Electronic Properties of Fluoroalkyl Groups. Fluorine p−π Interaction. *J. Am. Chem. Soc*. **1965**, *87* (11), 2410−2420.
(20) Saito, S.; Toriumi, Y.; Tomioka, N.; Itai, A. Theoretical Studies on *cis*-Amide Preference in *N*-Methylanilide. *J. Org. Chem*. **1995**, *60*, 4715−4720.
(21) King, M. T.; Reiss, P. D.; Cornell, N. W. Determination of Short-Chain Coenzyme A Compounds by Reversed-Phase High-Performance Liquid Chromatography. *Methods Enzymol*. **1988**, *166*, 70−79.
(22) Barr, R.; Lopaschuk, G. D. Measurement of Energy Metabolism in the Isolated Heart. In *Measurement of Cardiovascular Function*; McNeill, J. H., Ed.; CRC Press: New York, 1997; Chapter 2, pp 19−40.
(23) Reszko, A. E.; Kasumov, T.; David, F.; Thomas, K. R.; Jobbins, K. A.; Cheng, J.-F.; Lopaschuk, G. D.; Dyck, J. R. B.; Diaz, M.; Des Rosiers, C.; Stanley, W. C.; Brunengraber, H. Regulation of Malonyl-CoA Concentration and Turnover in the Normal Heart. *J. Biol. Chem.* **2004**, *279*, 34298−34301.
(24) Kolattukudy, P. E.; Poulose, A. J.; Kim, Y. S. Malonyl-CoA Decarboxylase from Avian, Mammalian, and Microbial Sources. *Methods Enzymol*. **1981**, *7*, 150−163.

JM050109N